MAGNETRON-SPUTTERED NANOCOMPOSITE nc-TiC/a-C COATINGS

Yu.S. BORISOV[1], **M.V. KUZNETSOV**[1], **A.V. VOLOS**[1], **V.G. ZADOYA**[1], **L.M. KAPITANCHUK**[1], **V.V. STRELCHUK**[2], **V.P. KLADKO**[2] and **V.F. GORBAN**[3]

[1]E.O. Paton Electric Welding Institute, NASU
11 Bozhenko Str., 03680, Kiev, Ukraine. E-mail: office@paton.kiev.ua
[2]V.E. Lashkaryov Institute of Semiconductor Physics, NASU
41 Nauka Ave., 03028, Kiev, Ukraine. E-mail: info@isp.kiev.ua
[3]I.M. Frantsevich Institute of Problems of Materials Science, NASU
3 Krzhizhanovsky Str., 03142, Kiev, Ukraine. E-mail: root@ipms.kiev.ua

One of the main directions in current progress of surface engineering is development of a nanocomposite structure, with at least one phase with less than 100 nm size of structural element among its components. Presence of a multiphase structure with dissimilar grain boundaries creates a barrier for their coarsening, thus providing stability of the formed coating structure. This work is devoted to investigation of the process of formation of a nanocomposite nc-TiC/a-C coating on substrates from 08Kh18N10T, Kh12M steels and VT1-0 titanium by the method of magnetron sputtering of graphite and titanium targets. In order to control the coating composition, a design procedure was developed, which envisages a change of power of magnetron discharge with titanium target at constant power of discharge with graphite target, that would allow producing coatings in the range of compositions of 42.5–70 at.% C and 57.5–30 at.% Ti. Coatings were studied by the methods of X-ray diffraction, Raman spectroscopy, X-ray photoelectron spectroscopy and microindentation. It is established that nanocrystalline TiC phase takes up 80 % and amorphous carbon matrix is 20 % of the coating structure. It is found that the degree of carbon ordering depends on coating composition. It is shown that the size of TiC grain and coating hardness depend on Ti/C ratio. Minimum size of TiC grain (2.9–4.3 nm) and maximum hardness (up to 30–38 GPa) are achieved at Ti/C ratio (in at.%) of 46/54. Maximum normalized hardness $H/E^* = 0.134$, which is the characteristic of coating material resistance to plastic deformation, is achieved on the substrate of 08Kh10N10T steel. 19 Ref., 3 Tables, 7 Figures.

Keywords: *nanocomposite coating, magnetron sputtering, titanium carbide, amorphous carbon, grain size, structure, hardness*

One of the main directions in current progress of materials science and surface engineering is use of nanostructural state of consolidated materials and coatings. This is due to the possibility of realization of dimensional effects, arising at refinement of structure grain to 100 nm and less, and accompanied by an essential change of mechanical, thermal, kinetic, electrical, magnetic and optical characteristics of materials [1–4].

However, practical application of materials and coatings with a totally nanosized structure is confronted with the problem of stability of such a structure, grain growth caused both by natural ageing and by the impact of external factors, namely mechanical, thermal, radiation, etc. This leads to the material loosing the specific properties, inherent to the nanocrystalline structural state.

Therefore, another direction of application of the advantages of nanostructural state of materials and coatings, being actively developed now, is creation of a nanocomposite structure, which has at least one phase with structural element size of less than 100 nm among its components [4]. Multiphase nature of the structure with dissimilar grain boundaries prevents grain coarsening that ensures the stability of the formed coating structure. It is established that owing to specifics of their structure, nanocomposites are characterized by improved physico-mechanical and catalytic properties [4].

Among nanocomposite coatings applied by vacuum deposition, a special place belongs to the group of coatings produced by the method of magnetron sputtering. Their structure consists of practically noninteracting phases with average size of structural elements below 100 nm [5–8]. Such structural elements are the amorphous matrix and nanocrystalline phase inclusions. Structural schematic of such a nanocomposite structure, which is synthesized by deposition of flows from several targets on the substrate in the atmosphere of reactive gases, is shown in Figure 1.

The best studied are such systems of nanocomposite structures as Me–C, Me–Si–N, where the amorphous matrix is carbon or Si_3N_4 with solid inclusions, mainly of carbides and nitrides of titanium, zirconium and chromium [9–11].

A number of research efforts were devoted to studying the influence of the composition of magnetron nc-TiC/a-C coating on nanosized nature of their structure, mechanical and tribotechnical properties [11–14]. In [13], at production of nc-TiC/a-C coating by magnetron sputtering of targets from compressed TiC and C mixtures in the proportion of 70/30, 50/50 and 30/70 (in mol.%), the coating, deposited by sputtering of 50/50 target, is a nanocomposite one at TiC grain size in the range of 6–11 nm and has hardness *HV*0.05-4190. When 30/70 target is used, coating structure is completely X-ray amorphous, and the authors classified it as metal-containing coating from amorphous carbon. Measurement of tribotechnical properties showed that TiC/C coating produced from 30/70 TiC/C target has the best characteristics. Friction coefficient under dry friction conditions on 100St6 steel was equal to 0.08–0.14 (at 0.4–0.5 for other coating compositions).

Evaluation of the influence of a-C amorphous phase content in the ranges from 0 to 100 % on the structure and mechanical properties of TiC/C coatings, produced at magnetron sputtering of titanium and graphite targets, demonstrated an increase of coating hardness from 17 up to 22 GPa at variation of its amount from 0 up to 45 %. At further increase of a-C-phase content lowering of hardness is observed, but coating tribological characteristics are improved. The best result was achieved at 65 % content, when the friction coefficient was below 0.2, wear rate was about 10^{-7} $mm^3/(N{\cdot}m)$ at coating hardness of 10–15 GPa [14].

Work [15] is a study of the influence of the composition of magnetron-sputtered TiC/a-C, WC/a-C and TiBC/a-C nanocomposite coatings on their structure and tribotechnical properties. In the case of TiC/a-C, the composition was varied within the range of content (in at.%) of 43.6–85.5 C; at WC/a-C it was 33.9–72.5, and at TiBC/a-C it was 31.2–71.3 C. A refinement of hard inclusion grain was observed in carbide-containing systems (from 30 to 2–3 nm for TiC, and from 9 to 2–3 nm for WC). TiBC grain in the case of 49.2–71.3 at.% C had the size of 2–3 nm. TiC/a-C, and WC/a-C nanocomposite coatings improve their tribomechanical properties at increase of carbon content with lowering of friction coefficient (from 0.31 to 0.04 for TiC/a-C, and from 0.84 to 0.19 for WC/a-C) and of the degree of wear, with lowering of coating hardness (from 22.3 to 8 GPa for TiC/a-C, and from 35.7 to 15.8 GPa for WC/a-C).

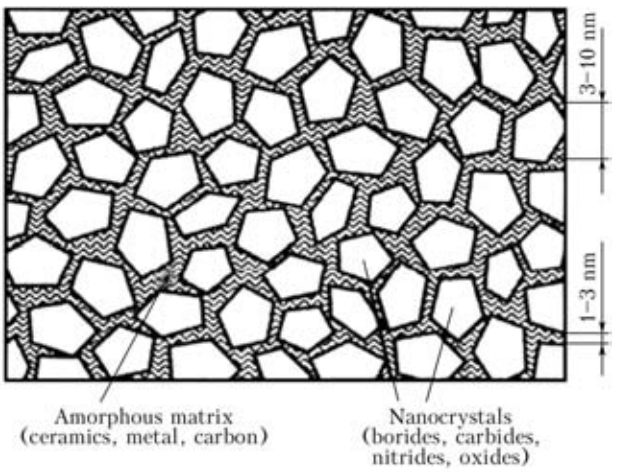

Figure 1. Schematic of nanocomposite structure

Similar results were presented in [16] and [17]. In [16] formation of X-ray amorphous phase at not less than 8 at.% Ti in the coating and of nanocomposite structure at 16 at.% Ti was confirmed. Coarsening of TiC grain from 5 up to 16 nm in the range of TiC content of 16–48 at.% and achievement of maximum hardness of 31 GPa at 30 at.% TiC was noted.

Work [17] is a study of the influence of carbon content on mechanical characteristics of nc-TiC/a-C coating in the range of 55–95 at.% C. It is shown that at content in the ranges of 70–95 at.% C, the index of normalized hardness H/E^* (E^* is the contact modulus of elasticity) was equal to 0.10–0.15, rising with increase of carbon content (%).

This work was devoted to investigation of the process of formation of nanocomposite TiC/C coating under the conditions of magnetron sputtering of separate targets from graphite and titanium, studying the influence of coating composition on its structure and mechanical properties.

Experimental and investigation procedures. The coating was deposited in an upgraded vacuum system VU-1BS, which was fitted with DC magnetron sputtering module consisting of two magnetrons: Magnetron 1 with a disc target (88 mm diameter, 4 mm thickness) from MPG-7 graphite of 99.98 % purity, and Magnetron 2 with a rectangular target (90 × 58 × 4 mm) from VT1-0 titanium (Figure 2). Magnetrons are mounted on one flange so that the angle between the target surfaces was equal to 150°. This enabled simultaneous or alternating deposition of coatings on a stationary substrate from two mag-

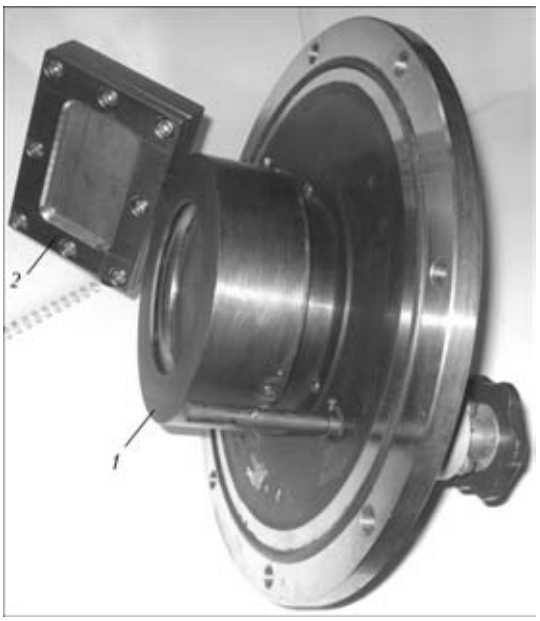

Figure 2. Module of magnetron sputtering, consisting of Magnetron 1 (*1*) and Magnetron 2 (*2*)

netrons with the same substrate-to-target distance equal to 110 mm.

Samples from 08Kh18N10T steel and VT1-0 titanium of 65 × 30 × 0.5 mm size, and Kh12M steel samples of 25 mm diameter and 6 mm thickness were used.

Before placing into the vacuum chamber, the sample was cleaned in an ultrasonic bath, successively filled with acetone and ethyl alcohol. In the vacuum at the pressure of $5 \cdot 10^{-4}$ Pa the sample was heated at 150 °C for 20 min, then without switching off the heater, sample surface was cleaned by argon ion bombardment in a glowing DC discharge at 1.3 Pa, 1100 V for 20 min. The coating was deposited in argon at working pressure of 0.4 Pa.

The process of forming TiC/C coating on the sample surface (with roughness Ra = 0.045 μm) consisted of two stages: deposition of an bond coat of titanium of 0.26–0.13 μm thickness with Magnetron 2 in the mode with negative voltage bias on the substrate at bias potential U_b = –100 V, and deposition of TiC/C coating (δ = 1.5–3.0 μm) using two magnetrons at U_b = 0 V. Here, carbon was deposited at constant values of specific power of magnetron discharge ΔP_1 = = 8.5 W/cm^2 and carbon deposition rate V_C = = 0.6 μm/h. Value of discharge power P_2 required to produce the specified percentage of titanium content in the coating was set on Magnetron 2.

To assess the power of Magnetron 2, required to produce the specified titanium content in TiC/C coating, a calculation procedure was developed, which consisted of the following stages:

1. Titanium content in the coating (at.%) C_{Ti}^{at}, proceeding from the known deposition rates of both the coating components (titanium and carbon), will be equal to

$$C_{Ti}^{at} = \frac{V_{Ti}}{V_{Ti} + V_C} \cdot 100; \quad (1)$$

2. Experimental determination of velocity of carbon coating atom deposition (C at/h) V_C with Magnetron 1 on the surface of reference sample across coating thickness, measured with a profile measurement device:

$$V_C = \frac{Q_C N}{A_C}, \text{ C at./h}, \quad (2)$$

where $Q_C = \delta_c \rho_c s$ is the carbon deposition rate, g/h ($\delta_c = 0.6 \cdot 10^{-4}$ cm/h — coating thickness; ρ_c = 2.2 g/cm^3 — electrode density; s = = 14.5 cm^2 — sample area; N = = $6.02 \cdot 10^{23}$ at/mole is the Avogadro number; A_C = 12.01 is the carbon atomic weight;

$$V_C = \frac{\delta_c \rho_c N s}{A_C} = 0.94 \cdot 10^{20}, \text{ C at/h}. \quad (3)$$

3. Experimental determination of the rate of titanium deposition at nominal power of Magnetron 2, equal to 325 W. Similar to previous calculation procedure

$$V_{Ti}^{nom} = \frac{\delta_{Ti} \rho_{Ti} N s}{A_{Ti}} = 1.27 \cdot 10^{20}, \text{ Ti at/h}, \quad (4)$$

where $\delta_{Ti} = 1.56 \cdot 10^{-4}$ cm; ρ_{Ti} = 4.5 g/cm^3, A_{Ti} = = 47.9.

4. As at magnetron sputtering the coating deposition rate is directly proportional to magnetron discharge power, at constant V_C the required V_{Ti}^w depends on working power of Magnetron 2 P_2^w, referred to the value of nominal power 325 W, where V_{Ti}^{nom} is known, i.e. $V_{Ti}^w / V_{Ti}^{nom} = P_2^w / P_2^{nom}$;

$$P_2^w = P_2^{nom} \frac{V_{Ti}^w}{V_{Ti}^{nom}} = V_{Ti}^w \frac{P_2^{nom}}{V_{Ti}^{nom}}, \text{ W}. \quad (5)$$

Proceeding from expressions (1) and (5)

$$V_{Ti}^w = \frac{C_{Ti}^{at} V_C}{100 - C_{Ti}^{at}}, \quad P_2^w = \frac{P_2^{nom}}{V_{Ti}^{nom}} \frac{C_{Ti}^{at} V_C}{100 - C_{Ti}^{at}}. \quad (6)$$

Using available data on V_C and V_{Ti}^{nom}, we obtain:

$$P_2^w = 240.5 \frac{C_{Ti}^{at}}{100 - C_{Ti}^{at}}, \text{ W}. \quad (7)$$

Figure 3 gives the graphic image of the obtained connection of titanium content in the coating with working power of Magnetron 2.

Phase analysis of coatings was conducted by the method of X-ray diffraction, using X-ray diffractometer Philips X'Pert — MPD with CuK_α X-ray source (wave length λ = 0.15418 nm). X-ray diffractograms (XD) were taken in sliding geometry (2θ scanning): angle of incident beam did not change and was equal to 4° relative to sample surface; full angular range of diffraction spectrum recording by 2θ = 20–80°, minimum step of 0.02°. Proceeding from analysis of XD spectra, the following parameters were determined: coating phase composition; average size of TiC phase grains (D); magnitude of average strain in TiC layer (ε).

Method of Raman spectroscopy was used for determination of configurations of carbon chemical bonds in the coating. Spectra of Raman scattering (RS) were measured in reflection geometry at room temperature, using triple Raman spectrometer T-64000 Horiba Jobin-Yvon, fitted with cooled CCD detector. Ar-Kr line of an ion laser with 488 nm wave length was used for excitation. Radiation was focused on the sample into a spot of 1 μm size, and power radiation hitting the sample was about 1 mW.

Ratios of carbon and TiC phases in TiC/C coating were determined by the method of X-ray photoelectron spectroscopy, using a high resolution electron spectrometer RIBER LAS 2000.

Determination of mechanical characteristics of coatings was conducted by the method of microindentation, using Micron-Gamma indentor [18]. Values of the characteristics were calculated automatically to ISO 14577-1:2002 standard.

Results and their discussion. Main characteristics of nc-TiC/a-C coatings of various composition deposited on substrates from 08Kh18N10T steels, as well as parameters of their deposition process, are given in Table 1.

As is seen from Table 1, in order to increase carbon content in TiC coating from 42.5 to 70 at.%, titanium deposition rate was reduced 3 times (at V_C = 0.6 μm/h). With increase of carbon content in the coating up to 54 at.% its hardness rises. For instance, in 8TiC (42.5 at.% C) and 19TiC (54 at.% C) samples hardness is equal to 7.7 and 17.5 GPa, respectively. At higher carbon content coating hardness decreases. Thus, changing the velocity of titanium target sputtering at preservation of optimum rate of carbon deposition allows controlling the composition and hardness value of the produced TiC/C coating.

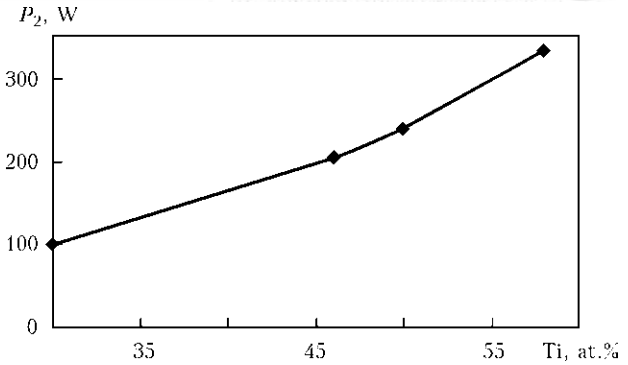

Figure 3. Dependence of required power of Magnetron 2 on required titanium content in TiC/C coating

Figure 4 gives XD of 8TiC, 19TiC and 26TiC samples with the respective Tables, which show lattice parameters, interplanar spacings, as well as crystal dimensions for each reflex.

Analysis of XD spectra shows that in the case of 8TiC and 19TiC samples a polycrystalline nanostructure with TiC crystal dimensions of 10.2–5.3 and 4.3–2.9 nm, respectively, forms in TiC/C coatings. With increase of carbon content in the coating, nanocrystal dimensions become smaller, and in 26TiC sample (70 at.% C) TiC phase is not found at all. As (111), (200), (220) and (311) reflexes are visible in the spectra, this is indicative of absence of any privileged direction of crystal growth.

Nanocrystalline structure of TiC/C coating (δ = 3 μm) studied by SEM at ×10,000 and ×100,000 magnification is shown in Figure 5, where TiC grains of 10–30 nm size are observed.

Structure of nc-TiC/a-C coatings is revealed by the spectrum of photoelectrons, generated under the impact of monochromatic X-ray radiation on the coating surface (Figure 6).

The spectrum has a wider carbon peak C1s, which is decomposed into two peaks of electrons with bond energies of 284.4 (*1*) and 281.2 (*2*) eV, corresponding to the presence of carbon phases and TiC in the coating. The ratio of values of peaks (*1*) and (*2*) shows that the phase of

Table 1. Parameters of magnetron deposition process and characteristics of nanocomposite nc-TiC/a-C coatings

Sample	Calculated coating composition, at.%	Titanium deposition rate, μm/h	TiC deposition rate, μm/h	Coating thickness δ, μm	Hardness H, GPa
8TiC	42.5 C 57.5 Ti	1.56	2.16	2.4	7.7
14TiC	50 C 50 Ti	1.05	1.65	1.9	8.0
19TiC	54 C 46 Ti	0.81	1.40	1.8	17.5
26TiC	70 C 30 Ti	0.50	1.10	1.2	15.7

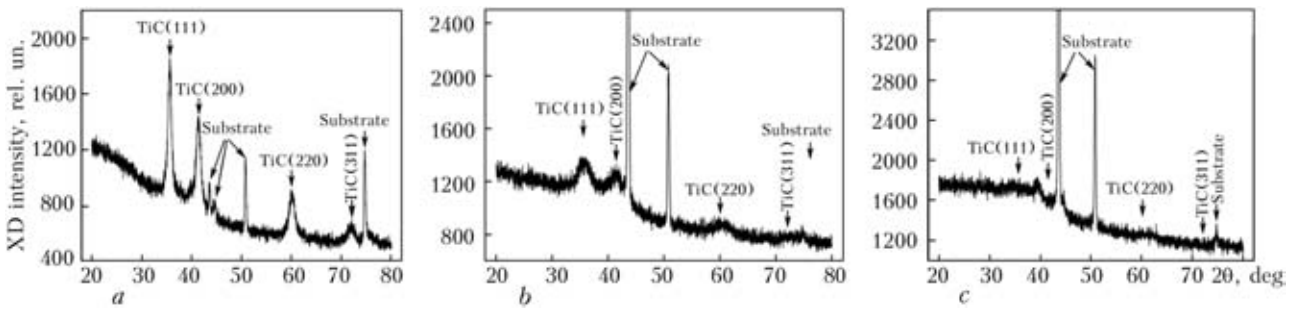

8TiC			
Reflexes	Interplanar space d, nm	Lattice constant, nm	Crystallite size, nm
(111)	0.2518	0.436	10.2
(200)	0.2180	0.436	8.1
(220)	0.1539	0.435	6.2
(311)	0.1312	0.435	5.3

19TiC			
Reflexes	Interplanar space d, nm	Lattice constant, nm	Crystallite size, nm
(111)	0.2519	0.436	3.4
(200)	0.2183	0.436	4.3
(220)	0.1535	0.434	2.9

Figure 4. X-ray diffractograms of TiC/C coatings of various composition, at.%: *a* — 8TiC (42.5 C; 57.5 Ti); *b* — 19TiC (54 C; 46 Ti); *c* — 26TiC (70 C; 30 Ti)

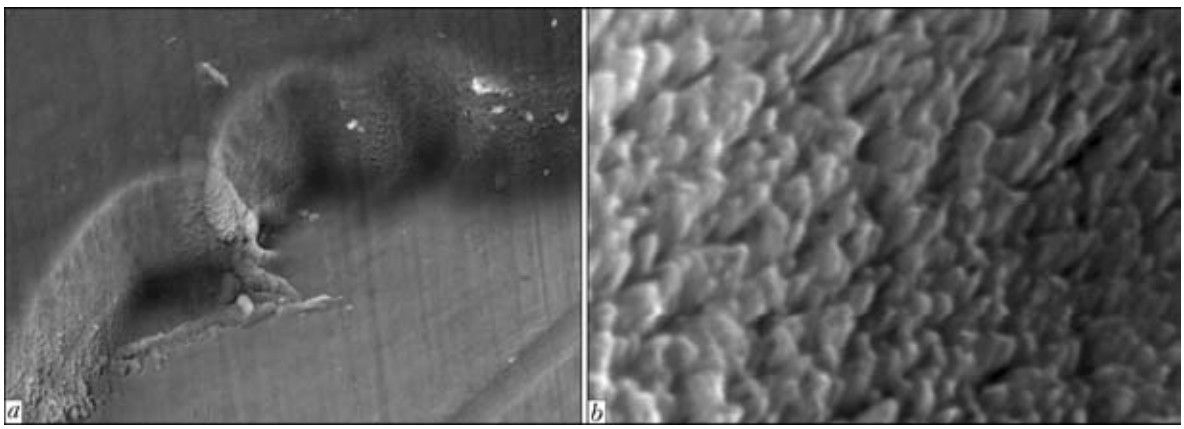

Figure 5. Microstructure of nc-TiC/a-C coating: *a* — ×10,000; *b* — ×100,000

nanocrystalline tungsten carbide TiC takes 80 % in the coating and 20 % is the amorphous carbon matrix.

Amorphous carbon state in nc-TiC/a-C coating is assessed by Raman scattering spectra (Figure 7).

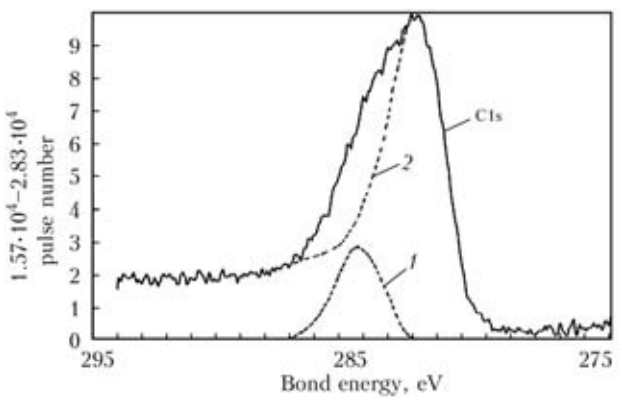

Figure 6. Spectrum of photoelectrons of nc-TiC/a-C coating (for designations see the text)

In the spectra of all the samples two Raman scattering bands are observed, which are characteristic for the state of carbon with sp^2- and sp^3-

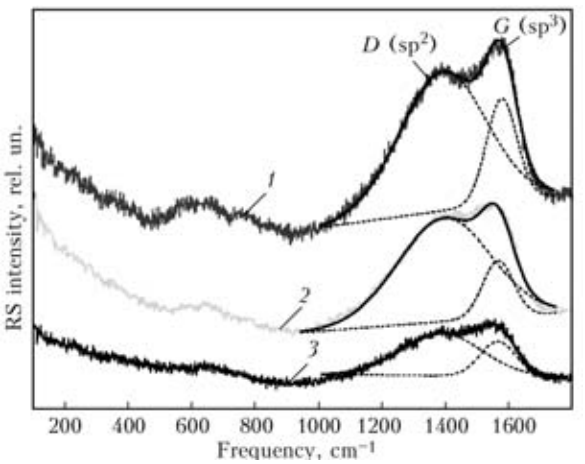

Figure 7. Spectra of Raman scattering on nc-TiC/a-C coatings of various composition: *1* — 8TiC; *2* — 19TiC; *3* — 26TiC

Table 2. Frequency positions (ω), pulse duration on half-amplitude level (FWHM), intensity ratio for *D* and *G* bands (I_D/I_G) evaluated by RS spectra of studied structures (acc. Figure 7)

Sample (coating composition, at.%)	*D*-band (sp^2)			*G*-band (sp^3)			I_D/I_G
	ω, cm^{-1}	FWHM, cm^{-1}	*I*, pulse	ω, cm^{-1}	FWHM, cm–1	*I*, pulse	
8TiC (42.5 C, 57.5 Ti)	1392.3	322.5	538.5	1577.7	113.1	403.4	1.33
19TiC (54 C, 46 Ti)	1397.0	346.7	396.9	1566.1	114.2	219.7	1.68
26TiC (70 C, 30 Ti)	1386.9	296.8	165.4	1565.4	132.6	134.5	1.23

Table 3. Mechanical properties of nc-TiC/a-C coatings (δ = 3.2 μm) on substrates from 08Kh18N10T and Kh12M steels

Sample, substrate	Hardness *H*, GPa	Contact modulus of elasticity E^*, GPa	Normalized hardness, H/E^*, GPa	Modulus of elasticity *E*, GPa	Stress of out-of-contact elastic strain σ_{es}, GPa	Coating composition, at.%	Grain size *D*, nm
29TiC, 08Kh18N10T	38.0	291	0.134	375	11.89	54 C, 46 Ti	2.9–4.3
30TiC, Kh12M	30.5	266	0.114	333	22.60	54 C, 46 Ti	2.9–4.3

hybridization of carbon electronic orbitals (bonds). *G* band of Raman spectrum with sp^3 bond is due to the presence of an ordered graphite phase. *D* band of the spectrum with sp^2 bond is characterized by structurally disordered graphite. Gauss approximating functions were used to perform decomposition of *G* and *D* band shapes into components, and ratio of band intensities I_D/I_G was determined. This ratio characterizes the proportion of graphite phases and is inversely proportional to the value of sp^3-phase fraction in the coating [19]. Therefore, the most ordered amorphous carbon with greater content of sp^3-phase is found in nc-TiC/a-C coatings on 8TiC and 26TiC samples, in which the smallest values of I_D/I_G ratio are equal to 1.33 and 1.23 (Table 2).

Microindentation method [18] was used to measure the mechanical properties of coatings on substrates from 08Kh18N10T and Kh12M steels (Table 3).

High hardness of the coating (30.5–38.0 GPa), according to the data of other researchers [14], is related to its low content of the amorphous phase (a-C = 20 at.%). Normalized hardness values H/E^* allow evaluation of the level of coating resistance to plastic deformation, which rises with increase of H/E^*, which is an index of coating material wear resistance.

Conclusions

1. Method of simultaneous DC magnetron sputtering of graphite and titanium targets on to substrates from 08Kh18N10T, Kh12M steels and titanium VT1-0 was used to produce at deposition rate of 1.4–2.2 μm/h a nanocomposite nc-TiC/a-C coating 2–3 μm thick with TiC inclusions of 3–10 nm size in an amorphous carbon matrix.

2. A procedure was developed for controlling nc-TiC/a-C coating composition by variation of power of magnetron discharge with a titanium target at constant power of the discharge with graphite target, thus ensuring the possibility of producing coatings in the composition range of 42.5–70 at.% C and 57.5–30 at.% Ti.

3. It is shown that the size of TiC grain and coating hardness depend on Ti/C ratio. Minimum size of TiC grain (2.9–4.3 nm) and maximum hardness (up to 30–38 GPa) are achieved at Ti/C ratio (in at.%) of 46/54.

4. Methods of Raman and photoelectronic spectroscopy were used to study the fine structure of nc-TiC/a-C coatings. It is found that TiC takes 80 % of the coating structure and 20 % is amorphous carbon matrix. It is shown that the degree of amorphous carbon ordering as to the content of sp^3-phase depends on coating composition.

5. Method of microindentation was used to determine the mechanical properties of nc-TiC/a-C coatings produced on various substrates. It is shown that the maximum normalized hardness of 0.134, which is a characteristic of coating material resistance to plastic deformation, was achieved on a substrate from 08Kh18N10T steel.

1. Andrievsky, R.A. (2001) Nanostructural materials: State, development and prospects. *Poroshk. Metallurgiya*, **6**, 5–11.
2. Andrievsky, R.A., Glezer, A.M. (1999) Dimensional effects in nanocrystalline materials. Pt 1: Peculiarities of structures. Thermodynamics. Kinetic phenomena. *Fizika Metallov i Metallovedenie*, 88(**1**), 50–73.
3. Andrievsky, R.A., Glezer, A.M. (2000) Dimensional effects in nanocrystalline materials. Pt 2: Mechanical and physical properties. *Ibid.*, 89(**1**), 91–112.

4. Ragulya, A.V., Skorokhod, V.V. (2007) *Consolidated nanostructural materials*. Kiev: Naukova Dumka.
5. Reshetnyak, E.N., Strelnitsky, V.E. (2008) Synthesis of reinforced nanostructural coatings. In: *Voprosy Atomnoj Nauki i Tekhniki.* Series Physics of radiation damages and radiotive materials sci., 92**(2)**, 119–130.
6. Shtansky, D.V., Levashov, E.A. (2009) Multicomponent nanostructural thin films: Problems and solutions (Review). *Izvestiya Vuzov. Tsv. Metallurgiya*, **9**, 12–15.
7. Veprek, S., Zhang, R.F., Veprek, M.J.G. et al. (2010) Superhard nanocomposites: Origin of hardness enhancement properties and applications. *Surf. and Coat. Technol*, **204**, 1898–1906.
8. Zhang, S., Sun, D., Fu, Y. et al. (2003) Recent advances of superhard nanocomposite coatings: a review. *Ibid*., **167**, 113–119.
9. Zehnder, T., Patscheider, J. (2000) Nanocomposite TiC/a-C:H hard coatings deposited by reactive PVD. *Ibid*., **133/134**, 138–144.
10. Voevodin, A.A., Zabinski, J.S. (2000) Supertough wear-resistant coating with «chameleon» adaptation. *Thin Solid Films*, **370**, 223–231.
11. Galvan, D., Pei, Y.T., de Hosson, J.Th. (2006) Influence of deposition parameters on the structure and mechanical properties of nanocomposite coatings. *Surf. and Coat. Technol.*, **201**, 590–598.
12. Patscheider, J., Zehnder, T., Dieseren, M. (2001) Structure-performance relations in nanocomposite coatings. *Ibid*., **146/147**, 201–208.
13. Stuber, M., Leiste, H., Ulrich, S. (2002) Microstructure and properties of low friction TiC-C nanocomposite coatings deposited by magnetron sputtering. *Ibid*., **150**, 218–226.
14. Martinez-Martinez, D., Lopez-Cartes, C., Fernandez, A. (2009) Influence of microstructure on the mechanical and tribological behavior of TiC/a-C nanocomposite coatings. *Thin Solid Films*, **517**, 1662–1671.
15. Sanchez-Lopez, J.C., Martinez-Martinez, D., Abad, M.D. et al. (2009) Metal carbide/amorphous C-based nanocomposite coatings for tribological application. *Surf. and Coat. Technol.*, **204**, 947–953.
16. Zhang, S., Lamb Bui, X., Jiang, J. et al. (2005) Microstructure and tribological properties of magnetron sputtered nc-TiC/a-C nanocomposite. *Ibid*., **198**, 206–211.
17. Pei., Y.T., Galvan, D., de Hosson, J.Th. et al. (2005) Nanostructured TiC/a-C coatings for friction and wear resistant applications. *Ibid*., **198**, 44–50.
18. Firstov, S.A., Gorban, V.F., Pechkovsky, E.P. (2009) *New methodology of processing and analysis of results of automatic material indentation*. Kiev: Logos.
19. Ferrari, A., Robertson, J. (2000) Interpretation of Raman spectra of disordered and amorphous carbon. *Phys. Rev. B*, 61**(20)**, 14095–14107.

Received 28.05.2013